

## Article

# SYNTHESIS, STRUCTURAL AND PHOTOPHYSICAL PROPERTIES OF A NEW DITOPIC TERPYRIDINE-BASED PROLIGAND BEARING DISELENIDE UNITS

Adelina A. ANDELESCU<sup>1\*</sup>, Evelyn POPA<sup>1</sup>, Elisabeta-Ildyko SZERB<sup>1</sup>

<sup>1</sup>“Coriolan Drăgulescu” Institute of Chemistry, Romanian Academy, 24 Mihai Viteazu Blvd., 300223 Timisoara, Romania

**Abstract:** The present paper describes the synthesis and characterization of a new ditopic proligand with two terpyridines linked by a diselenide unit, obtained by a Steglich esterification procedure between a bis-carboxylic acid functionalized with a diselenide unit and 4-([2,2':6',2''-terpyridin]-4'-yl)phenol. The compound was characterized by FT-IR, NMR (1D and 2D) and UV-Vis spectroscopies and ESI-MS analysis. Moreover, the photophysical properties of the ditopic ligand were investigated in freshly prepared dichloromethane solution. The compound was found to be emissive with a maximum centered at 354 nm.

**Keywords:** heterocycles; N-donor ligand; ditopic ligand; oligopyridines;

## INTRODUCTION

The molecule 2,2':6',2''-terpyridine (*tpy*) is a tridentate ligand with three nitrogen coordination sites (Mughal et al. 2020) and was first reported in 1932 by Morgan and Burstall as one of 20 products of the reaction when they heated pyridine and anhydrous iron(III) chloride in an autoclave (Morgan and Burstall 1932).

Since then, *tpy* and its derivatives have received attention due to their ability to easily form metal complexes with main-group, *d*-block and lanthanide elements (Fallahpour 2002, Mughal et al. 2020). *Tpy* derivatives and their metal complexes have been studied in supramolecular chemistry and catalysis (Wey et al. 2019), electrochemical sensors (Negrea et al. 2022, Popa et al. 2023), as DNA binders and medicinal chemistry (Abhijnakrishna et al. 2023), etc.

Various synthetic procedures have been employed for the synthesis of *tpy* scaffolds (Fallahpour 2002, Kainat et al. 2024), such as cross-coupling [Li et al. 2011, Robo et al. 2014, Zibaseresht 2019] or ring assembly methods (Fernandes et al. 2018, Wang et al. 2019).

Among them, the one-pot Kröhnke reaction [Kröhnke 1976] is the most commonly employed method, and it involves the reaction of two equivalents of a substituted acetylpyridine derivative with an aldehyde in a basic medium and in the presence of an ammonia source. Following the Kröhnke

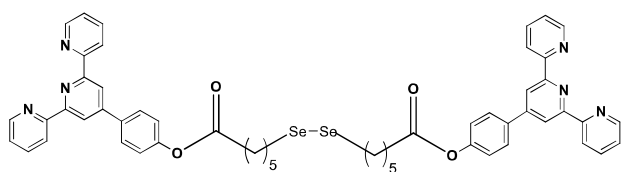
methodology, a wide variety of 4'-substituted *tpy* derivatives were reported (Kainat et al. 2024).

Ditopic ligands, with two different, separated metal-binding domains in their structures, can form two types of coordination compounds: homo and hetero multi-metallic complexes (Salimova et al. 2020, Schäfer et al. 2021)

The first of these are complexes in which both ligand fragments, coordinate the same metal ion. Polymetallic complexes may be obtained using ditopic terpyridinyl units resulting in luminescent materials or electrochemical sensors [Indelli et al. 1998, Andeleescu et al. 2024].

Moreover, the synthesis of ditopic *tpy* derivatives with an additional donor atom (such as: sulphur or selenium) is of interest due to their ability to bind nanoparticles (Yee et al. 2003, Rudakovskaya et al. 2010, Romashkina et al. 2013, Margandan et al. 2017, Popa et al. 2024). On this background, we report the synthesis and characterization of a new ditopic *tpy* proligand, namely bis(4-([2,2':6',2''-terpyridin]-4'-yl)phenyl)6,6'-diselenediyldihexanoate (Figure 1), which contains additionally an aromatic ring on its structure, compared to the one previously reported by our group (Popa et al. 2024). Also, the insertion of selenium atom into the structure may lead to compounds with potential applications as drugs (Banerjee et al. 2017). Due

to the presence of three nitrogen rings, the ditopic terpyridine-based ligand may find future applications as coordination polymers (Shu *et al.* 2022), whereas the presence of a diselenide unit enables them to be studied as drug delivery systems or anticancer drugs (Han *et al.* 2019). The compound was structurally characterized by FT-IR, NMR, and UV-Vis spectroscopies. The proposed structure is supported by the ESI-MS analysis. The photophysical properties of the final compound were investigated in freshly prepared dichloromethane solution.



Compound 3

Figure 1. Proposed chemical structure of the terpyridine derivative.

## MATERIALS AND METHODS

$N,N'$ -dicyclohexylcarbodiimide (DCC), 4-dimethylaminopyridine (4-DMAP), 2-acetylpyridine, 4-methoxybenzaldehyde, anhydrous THF, and DMF were purchased from Sigma Aldrich and used without any further purification. The solvents used for the column chromatography were purchased from Carlo Erba. Neutral  $Al_2O_3$  60 and spectrofluorimetric grade dichloromethane were purchased from VWR.

Melting point was determined by optical microscopy using an Olympus BX53M polarizing microscope (POM) equipped with a Linkam hot-stage. Infrared spectra (KBr pellets) in the range 4000-400  $cm^{-1}$  range were recorded on a Cary 630 FT-IR spectrophotometer.

The  $^1H$ -NMR spectra were recorded either on a Bruker Fourier 300 MHz spectrometer or Bruker Avance 300) in  $CDCl_3$  or  $DMSO-d_6$ . 1D and 2D NMR experiments were recorded on Bruker Avance III HD – 500 MHz spectrometer in  $CDCl_3$ .

Spectrofluorimetric grade dichloromethane was used for the photophysical investigations in solution. The absorption spectrum in solution was recorded on an Agilent Cary 60 spectrophotometer using quartz cuvettes of 1 cm path length. The emission spectrum were

recorded on Horiba Fluoromax Plus spectrofluorometer. The luminescence quantum yields of the samples in the solution were recorded using a QuantaPhi-2 integrating sphere with 121 mm internal diameter with reflectivity from 250 to 2500 nm.

High-resolution mass spectral (HRMS) spectra was recorded on Orbitrap IQ-X Mass Spectrometer from Thermo Scientific using an electrospray ionization (ESI) technique. The equipment was operated in positive-ion mode and ion transfer parameters were optimized to enable detection of ions in a  $m/z$  range between 150 and 2000. The employed parameters are listed in Table 1. The system was externally calibrated by using Pierce FlexMix Calibration Solution from Thermo Scientific. The data was collected in positive MS scan mode and processed using Thermo Scientific Xcalibur 4.7 software.

Table 1. Employed parameters for ESI-MS technique

Source parameters	Values
Ionization mode	Positive electrospray ionization
Spray voltage	3200 V
Sheath gas flow rate	5 Arb
Auxiliary gas flow rate	2 Arb
Sweep gas flow rate	0 Arb
Ion transfer tube temperature	300 °C
Vaporizer temperature	20 °C
Acquisition parameters	Values
Detector type	Orbitrap
Orbitrap resolution	120000
Scan range	400-1500 $m/z$
AGC target	100%
Injection time	100 ms
Syringe flow	5 $\mu$ l/min

## EXPERIMENTAL SECTION

*Synthesis of 4-([2,2':6',2''-terpyridin]-4'-yl)phenol, 2*

Compound 2 was obtained in two steps following a reported procedure (Bahrami *et al.* 2017) and the results agree well with the reported data.

**II**: white solid (0.91 g, 2.68 mmol, 65.6 %).

**FT-IR** (KBr,  $cm^{-1}$ ): 2992 ( $\nu$ (C-H)); 1600 – 1431 ( $\nu$  (C=N)) and ( $\nu$  (C=C)).

**$^1H$ -NMR** (300 MHz,  $CDCl_3$ ,  $\delta$ /ppm): 8.75 - 8.59 (m, 6H), 7.94-7.68 (m, 4H), 7.42-7.25 (m, 2H), 7.12-6.92 (m, 2H), 3.89 (s, 3H);

Compound **2**: pale grey solid (0.720 g, 2.21 mmol, 93 %).

**FT-IR** (KBr,  $\text{cm}^{-1}$ ): 3250 ( $\nu_{\text{OH}}$ , broad); 1616 – 1430 ( $\nu$  (C=N)) and ( $\nu$  (C=C)).

**$^1\text{H-NMR}$**  (300 MHz, DMSO- $d_6$ ,  $\delta/\text{ppm}$ ): 8.77-8.70 (d, 2H), 8.69-8.55(d, 4H), 8.07- 7.95 (td, 2H), 7.81 -7.60(m, 2H), 7.57- 7.43 (m, 2H), 7.00- 6.95(dd, 2H).

*Synthesis of bis(4-([2,2':6',2''-terpyridin]-4'-yl)phenyl) 6,6'-diselanediyldihexanoate, **3***

0.09 g (0.23 mmol) of compound **1**, 0.166 g (0.51 mmol) of compound **2** and 22.65 mg (0.1854 mmol) of 4-DMAP in 10 mL THF and 1 mL of DMF were stirred at room temperature under argon atmosphere for 30 minutes, then 0.105 g (0.51 mmol) of DCC in 3 mL of THF were added dropwise. The consumption of the starting materials was monitored on TLC ( $\text{Al}_2\text{O}_3$ :  $\text{CHCl}_3$ :hexane = 1:1). After 5 days, the reaction mixture was taken to dryness, dissolved in  $\text{CHCl}_3$ , washed with distilled water (3x50 mL), the organic phase was dried over anhydrous sodium sulfate, filtered and taken to dryness. The residue was taken with AcOEt and the undissolved precipitate was filtered (to remove the DCU biproduct) and mother liquor was taken to dryness. This procedure was repeated 3 times. The pure compound was isolated after purification on column chromatography using  $\text{Al}_2\text{O}_3$  as stationary phase in  $\text{CHCl}_3$ :hexane = 1:1, resulting in a yellow gel (0.058 mmol, 25%).

**Melting point**: 83-85°C.

**FT-IR** (KBr,  $\text{cm}^{-1}$ ): 1762 ( $\nu_{\text{C=O}}$ ); 1605 – 1412 ( $\nu$  (C=N)) and ( $\nu$  (C=C)).

**$^1\text{H-NMR}$**  (500 MHz,  $\text{CDCl}_3$ ,  $\delta/\text{ppm}$ ): 8.67 – 8.62 (m, 4H), 8.58 (dt,  $J = 7.9, 1.1$  Hz, 2H), 7.86 – 7.82 (m, 2H), 7.80 (td,  $J = 7.7, 1.8$  Hz, 2H), 7.27 (ddd,  $J = 7.5, 4.8, 1.3$  Hz, 2H), 7.18 – 7.15 (m, 2H), 2.90 (t,  $J = 7.4$  Hz, 2H), 2.55 (t,  $J = 7.4$  Hz, 2H), 1.81 – 1.71 (m, 4H), 1.50 (tdd,  $J = 9.9, 8.6, 5.1$  Hz, 2H).

**$^{13}\text{C-NMR}$**  (126 MHz,  $\text{CDCl}_3$ ,  $\delta/\text{ppm}$ )  $\delta$  171.88, 156.07, 155.88, 151.49, 149.38, 149.06, 136.99,

136.02, 128.46, 123.90, 122.11, 121.43, 118.83, 34.27, 30.60, 29.68, 28.92, 24.41.

**HR-MS** ( $\text{C}_{54}\text{H}_{48}\text{N}_6\text{O}_4\text{Se}_2+\text{H}$ ): simulated: 1005.21442, found: 1005.21402

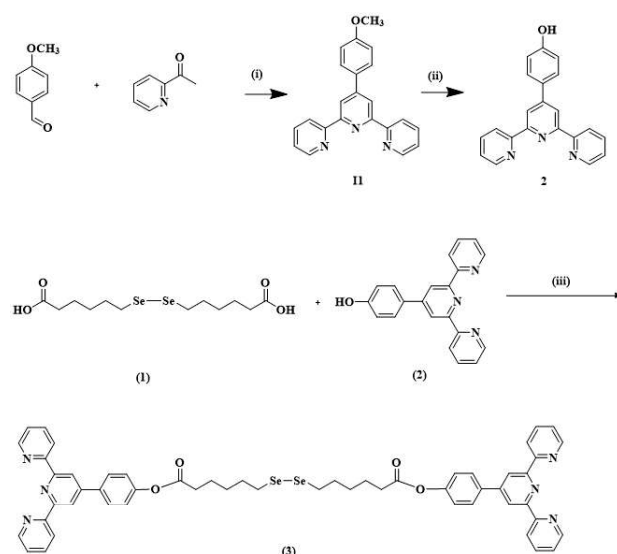
## RESULTS AND DISCUSSIONS

The preparation of compound **3**, required the synthesis of the starting materials: 6,6'-(1,2-diselanediyldihexanoic acid, **1** and 4-([2,2':6',2''-terpyridin]-4'-yl)phenol, **2**.

6,6'-(1,2-diselanediyldihexanoic acid, **1** was obtained and fully characterized in a previously published paper of our group [Popa *et al.* 2024].

For the synthesis of 4-([2,2':6',2''-terpyridin]-4'-yl)phenol, **2** a reported procedure was followed, which involved a one-pot Kröhnke condensation between 4-methoxybenzaldehyde and 2-acetylpyridine, in a basic media [Bahrami *et al.* 2017]. The pure compound was isolated after a recrystallization from methanol [Chen *et al.* 2018]. The intermediate **11** was then demethylated under strong acidic conditions to yield the desired compound **2**. The reaction pathway is presented in Scheme 1.

The desired compound **3**, bis(4-([2,2':6',2''-terpyridin]-4'-yl)phenyl) 6,6'-diselanediyldihexanoate was obtained adapting a procedure reported by our group (Scheme 1, Popa *et al.* 2024), through a Steglich esterification reaction between compound **1** and **2** equivalents of compound **2**, using DCC as a coupling reagent in the presence of 4-DMAP as catalyst.



Scheme 1. Reaction pathway for the synthesis of compounds **2** and **3**. Reagents and conditions: (i) KOH, EtOH, NH<sub>4</sub>OH, ΔT, 24 hours; (iii) DCC, 4-DMAP, THF-DMF (10-1 V/V), inert atmosphere, r.t, 5 days;

Compound **3** was isolated as a yellow waxy solid. Its structure was proposed based on spectroscopic methods: FT-IR, NMR (1D and 2D) spectroscopy and MS spectrometry.

The first confirmation of the formation of the desired compound **3**, was gained from FT-IR analysis through the shift of the characteristic absorption band of the carbonyl group ( $\nu_{C=O}$ ) from 1694 cm<sup>-1</sup> in compound **1**, to 1762 cm<sup>-1</sup> in compound **3**, which is characteristic of the C=O bond in esters. Moreover, the stretching vibration of the  $\nu_{C-Se}$  bond is identified at 635 cm<sup>-1</sup> in compound **1**, and 640 cm<sup>-1</sup> in compound **3** (Helios et al. 2015). The main characteristic absorption bands of the compound are reported in Table 2.

Table 2. Assignment of the characteristic absorption bands of the starting materials and the final compound **3**.

Cpd	Assignment of the characteristic absorption bands (wavenumber values in cm <sup>-1</sup> )		
	$\nu_{C=O}$	$\nu_{C=N \text{ and } C=C}$	$\nu_{C-Se}$
<b>1*</b>	1694	-	635
<b>2</b>	-	1616 – 1430	-
<b>3</b>	1762	1605 – 1412	641

\* Data reported in Popa *et al.* 2024

In order to confirm the proposed structure, 1D and 2D NMR spectra were recorded on a Bruker 500 MHz instrument. This allowed us to fully index all the protons and carbon atoms based on <sup>1</sup>H-<sup>1</sup>H COSY (Correlation Spectroscopy), HSQC (Heteronuclear Single Quantum Coherence), and HMBC (Heteronuclear Multiple Bond Correlation) experiments. The results are summarized in Table 3.

Table 3. 1D and 2D NMR data of compound **3** recorded in CDCl<sub>3</sub>

Atom label	<sup>1</sup> H	<sup>13</sup> C	COSY	HMBC
C	1.50 (tdd, $J = 9.9, 8.6, 5.1$ Hz, 2H)	28.92	B,D	A, D, E
B, D	1.81 – 1.68, m, 4H	30.60 (B), 24.41 (D)	A,E,C	A, D, E, F,

E	2.55, t, $J = 7.4$ Hz, 2H	34.27	D	D,C,F
A	2.90 (t, $J = 7.4$ Hz, 2H),	29.68	B	-
F	-	171.88	-	-
1*	8.67 – 8.62 (m, 4H)	149.06	2	2, 3
2	7.27 (ddd, $J = m, 2H$ )	123.90	1, 3	1, 4, 5, 6
3	7.80 (td, $J = 7.7, 1.8$ Hz, 2H)	136.99	1, 2	1, 4, 6
4	8.58 (dt, $J = 7.9, 1.1$ Hz, 2H)	121.43	3	2, 5, 6
5	-	155.88	-	-
6	-	156.07	-	-
7*	8.67 – 8.62 (m, 4H)	118.83	-	4, 5, 6, 9, 11,
8	-	149.38	-	-
9	-	136.02	-	-
10	7.86 – 7.82 (m, 2H)	128.46	11	8, 11, 12
11	7.23 – 7.08 (m, 2H)	122.11	10	9, 12
12	-	151.49	-	-

\* Peaks appear overlapped in <sup>1</sup>H-NMR spectra in total 4H

The <sup>1</sup>H-NMR spectrum (Figure 2) presented all the expected signals of the protons, and their integration agrees with the proposed structure, while the <sup>13</sup>C-NMR spectra contained all the expected signals for the 18 carbon atoms from half of the molecule.

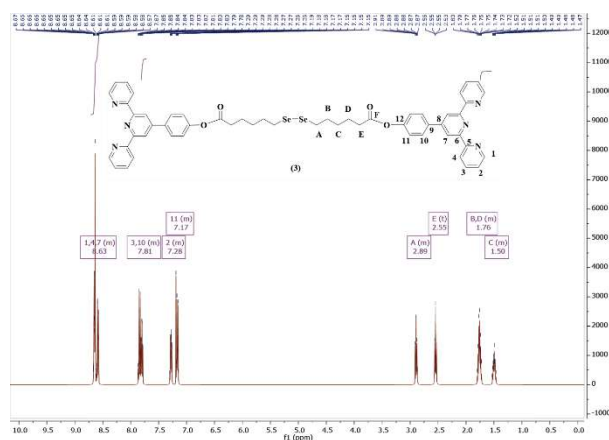


Figure 2. The <sup>1</sup>H-NMR spectrum of compound **3** recorded in CDCl<sub>3</sub> and the atom labeling.

Finally, the proposed structure is supported by the ESI-MS analysis (Figure 3).

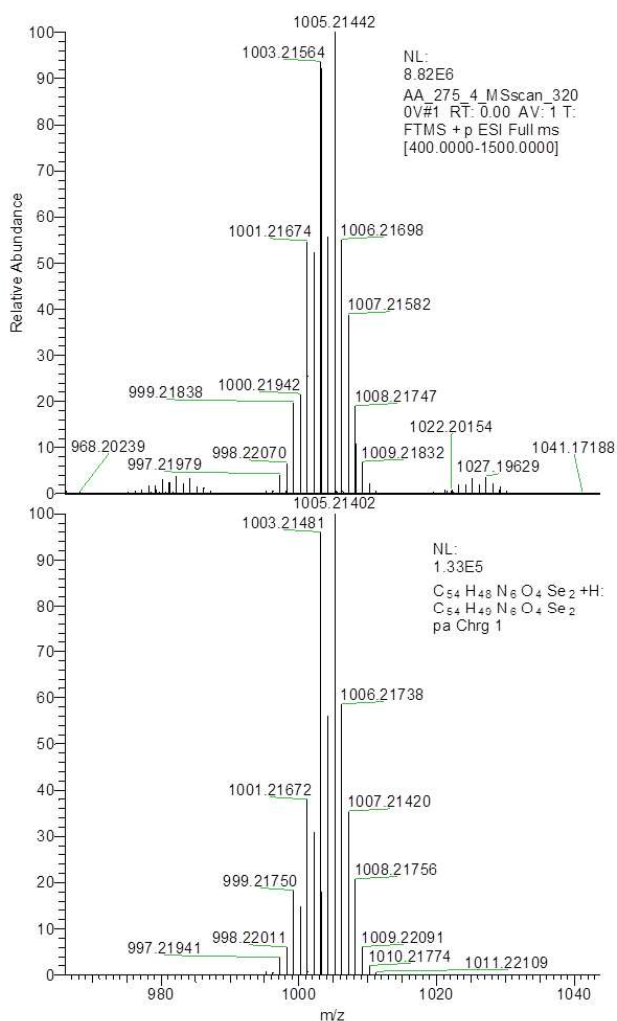


Figure 3. Simulation vs. experimental MS spectra for compound **3**.

The photophysical properties of compound **3** (absorption, emission maxima and lifetimes of the excited states) were determined in freshly prepared dichloromethane solution and the data are presented in Figure 4 and summarized in Table 4. From the absorption spectra several information could be obtained: the absorptions band from 252 and 280 nm are due to  $\pi\text{-}\pi^*$  from the *tpy* ring (Toledo et al. 2015), whereas the shoulder centered at 311 nm may be due to the diselenide bond (Back et al. 1983). It is well known that the *tpy* scaffolds present fluorescence properties at room temperature (Costa et al. 2015), therefore the emission spectrum was recorded after excitation at 311 nm, presenting an emission band centered 354 nm.

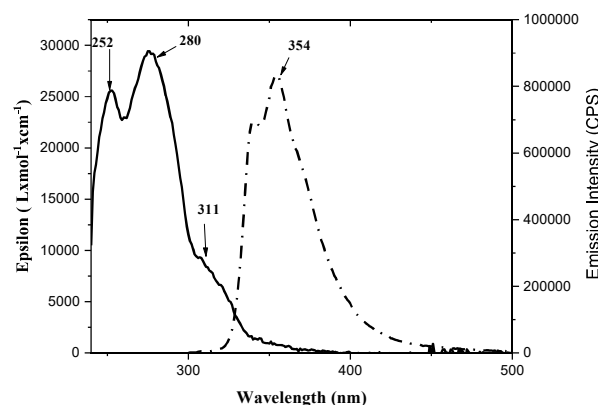


Figure 4. Absorption (solid line) and emission (dashed line) of compound **3** in  $\text{CH}_2\text{Cl}_2$  solution ( $c= 5 \cdot 10^{-6}$  mol/L).

Table 4. Photophysical properties of compound **3** in solution ( $c= 5 \cdot 10^{-6}$  mol/L).

Sample	Abs, $\lambda_{\text{max}}/\text{nm}$ ( $\epsilon/\text{M}^{-1} \text{cm}^{-1}$ )	Em, $\lambda_{\text{max}}/\text{nm}$	$\phi$ /%
1*	308 (640)	-	-
2**	286, 330-410	384	-
3	252 (25512) 280 (29364) 311 (9077)	354 ( $\lambda_{\text{ex}}=311$ nm)	6.33

\* Data reported by Popa *et al.* 2024

\*\* Data recorded in ethanol solution reported by Sierra *et al.* 2018

Structurally similar terpyridine ligands with disulfide moieties were reported by Majouga *et al.* 2010, but their photophysical properties were not investigated, whereas in case of those with diselenide units, there is only one reported by our group (Popa *et al.* 2024) with its emission maxima centered at 349 nm. Compared to the compound reported in the present paper it presents a small bathochromic shift of 5 nm. The compound presented a quantum yield value of 6.33 %.

Recently it was mentioned that linear diselenides quenched fluorescence through a synergistic combination of intramolecular charge transfer, ICT and Förster resonance energy transfer, FRET (Ma et al. 2024). Therefore, the low quantum yield value may be attributed to the quenching effect of the diselenide moiety.

## CONCLUSIONS

A new terpyridine derivative containing a diselenide unit was obtained and its structure was confirmed based on FT-IR, NMR (1D and

2D) investigations and HR-MS spectrometry. Its optical properties were investigated in freshly prepared dichloromethane solutions by UV-Vis and fluorescence measurements.

#### ACKNOWLEDGEMENTS

This work was supported by a grant of the Ministry of Research, Innovation and Digitization, CNCS/CCCDI – UEFISCDI, project number PN-III-P1-1.1-PD-2021-0427, within PNCDI III.

Authors acknowledge the Romanian Academy, Program 4 and the infrastructure support granted by the project RO-OPENSSCREEN, MySMIS code: 127952, Contract no. 371/20.07.2020, co-financed by European Regional Development Fund through the Competitiveness Operational Program 2014-2020.

#### REFERENCES

Andelescu, A.A, Candreva, A., Popa, E., Visan, A., Cretu, C., La Deda, M., Szerb, E.I., 2024. Role of the Environment Polarity on the Photophysical Properties of Mesogenic Hetero-Polymetallic Complexes. *Molecules* 29, 750. <https://doi.org/10.3390/molecules29040750>

Abhijnakrishna, R., Magesh, K., Ayushi, A., Velmathi, S., 2023. Advances in the Biological Studies of Metal-Terpyridine Complexes: An Overview From 2012 to 2022. *Coordination Chemistry Reviews* 496, 215380. <https://doi.org/10.1016/j.ccr.2023.215380>

Bahrami, K., Khodaei, M.M., Meibodi, F.S., 2017. Suzuki and Heck cross-coupling reactions using ferromagnetic nanoparticle-supported palladium complex as an efficient and recyclable heterogeneous nanocatalyst in sodium dodecylsulfate micelles. *Applied Organometallic Chemistry* 31(6), e3627. <https://doi.org/10.1002/aoc.3627>

Back, T.G., Coddling, P.W., 1983. Studies of the dihedral angle of a crowded diselenide by X-ray crystallography and ultraviolet spectroscopy. *Canadian Journal of Chemistry* 61, 2749–2752. <https://doi.org/10.1139/v83-472>

Banerjee, B., Koketsu, M., 2017. Recent developments in the synthesis of biologically relevant selenium-containing scaffolds. *Coordination Chemistry Reviews* 339, 104–127.

Costa, J., Ruloff, R., Burai, L., Helm, L., Merbach, A.E., 2005. Rigid MIL2Gd2III (M ¼ Fe, Ru) complexes of a terpyridine-based heteroditopic chelate: a class of candidates for MRI Contrast agents. *Journal of the American Chemical Society* 1102, 5147-5157. <https://doi.org/10.1021/ja0424169>

Chen, F., Tian, Y.-K., Chen, Y., 2018. Controlled formation of main chain supramolecular polymer based on metal–ligand interaction and thiolene click reaction. *Chemistry - An Asian Journal* 13, 3169 – 3172. <https://doi.org/10.1002/asia.201801235>

Fernandes, S.S.M., Belsley, M., Ciarrocchi, C., Licchelli M., Raposo, M.M.M., 2019. Terpyridine derivatives functionalized with (hetero)aromatic groups and the corresponding Ru complexes: Synthesis and characterization as SHG chromophores. *Dyes and Pigments* 150, 49–58. <https://doi.org/10.1016/j.dyepig.2017.10.046>

Han, W., Zhang, S., Qian, J., Zhang, J., Wang, X., Xie, Z., Xu, B., Han, Y., Tian, W., 2019. Redox Responsive Fluorescent nanoparticles based on Diselenide-containing AIEgens for Cell imaging and Selective Cancer Therapy. *Chemistry - An Asian Journal* 14, 1745–1753. <https://doi.org/10.1002/asia.201801527>

Helios, K., Pietraszko, A., Zierkiewicz, W., Wójtowicz, H., Michalska, D., 2015. The crystal structure, infrared, Raman and density functional studies of bis(2-aminophenyl) diselenide. *Polyhedron* 30, 2466–2472. <https://doi.org/10.1016/j.poly.2011.06.040>

Kainat, S.F., Hawsawi, M.B., Mughal, E.U., Naeem, N., Almohyawi, A.M., Altass, H.M, Hussein, E.M., Sadiq, A., Moussa, Z., Abd-El-Aziz, A.S, Ahmed, S.A., 2024. Recent developments in the synthesis and applications of terpyridine-based metal complexes: a systematic review. *RSC Advances* 14, 21464-21537. <https://doi.org/10.1039/D4RA04119D>

Kröhnke, F., 1976. The Specific Synthesis of Pyridines and Oligopyridines. *Synthesis*, 1–24.

Li, J., Sato, T., Li, H., Higuchi, M., 2011. Synthesis of Unsymmetrical, Monosubstituted Bis-terpyridine Derivatives via Suzuki-Miyaura Cross-Coupling. *Synthesis* 9, 1361-1364.

Ma, T., Gao, H., Wu, J., Zhao, J., Chang, B., Zhang, Z., Zhang, S., Baoxin, Z., Fang, J.,

2024. Diselenides as novel effective fluorescence quenchers to construct a two-photon fluorescent probe for thiols in a mouse stroke model. *Chemical Communications* 61, 1910-1913. <https://doi.org/10.1039/D4CC06286H>
- Majouga, A.G., Romashkina, R.B., Kashaev, A.S., Rahimov, R.D., Beloglazkina, E.K., Zyk, N.V., 2010. New organic ligands of the terpyridine series: modification of gold nanoparticles, preparation of coordination compounds with Cu(I), catalysis of oxidation reactions. *Chemistry of Heterocyclic Compounds* 46, 1076–1083. <https://doi.org/10.1007/s10593-010-0630-y>
- Margandan, K., Jebastin, S.J.M., 2017. Synthesis And Characterization Of Bismercapto (2, 2':6', 2''-Terpyridine) Ru(II)-Complexes Stabilized Gold Nanoparticles And Their Electro Catalytic Reduction Of Nitrite. *Journal of the Chilean Chemical Society* 62(4), 3691-3699.
- Morgan, G.T., Burstall, F.H., 1932. Dehydrogenation of pyridine by anhydrous ferric chloride. *Journal of the Chemical Society, Abstracts*, 20-30. <https://doi.org/10.1039/JR9320000020>
- Mughal, E.U., Mirzaei, M., Sadiq, A., Fatima, S., Naseem, A., Naeem, N., Fatima, N., Kausar, S., Altaf, A.A., Muhammad, Z.N., Ahmad, K.B., 2020. Terpyridine-metal complexes: effects of different substituents on their physico-chemical properties and density functional theory studies. *Royal Society Open Science* 7 (11), 201208. <https://doi.org/10.1098/rsos.201208>
- Negrea, S., Andelescu, A.A., Ilies, S., Cretu, C., Cseh, L., Rastei, M., Donnio, B., Szerb, E.I., Manea, F., 2022. Design of Nanostructured Hybrid Electrodes Based on a Liquid Crystalline Zn(II) Coordination Complex-Carbon Nanotubes Composition for the Specific Electrochemical Sensing of Uric Acid. *Nanomaterials* 12(23), 4215. <https://doi.org/10.3390/nano12234215>
- Popa, E., Andelescu, A.A., Ilies (b. Motoc), S., Visan, A., Cretu, C., Scarpelli, F., Crispini, A., Manea, F., Szerb, E.I., 2023. Hetero-Bimetallic Ferrocene-Containing Zinc(II)-Terpyridyl-Based Metallomesogen: Structural and Electrochemical Characterization. *Materials* 16(5), 1946. <https://doi.org/10.3390/ma16051946>
- Popa, E., Andelescu, A.A., Badea, V., Svera, P., Szerb, E.I., 2024. Bis(2,6-di(pyridin-2-yl)pyridin-4-yl)-6,6'-(1,2-diselanediyldihexanoate. *Molbank* 2024(1), M1752. <https://doi.org/10.3390/M1752>
- Robo, M.T., Prinsell, M.R., Weix, D. J., 2014. 4,4',4''-Trimethyl-2,2':6',2''-terpyridine by Oxidative Coupling of 4-Picoline. *The Journal of Organic Chemistry* 79 (21), 10624–10628. <https://doi.org/10.1021/jo501925s>
- Rudakovskaya, P.G., Beloglazkina, E.K., Majouga, A.G., Zyk, N.V., 2010. Synthesis and characterization of terpyridine-type ligand-protected gold-coated Fe<sub>3</sub>O<sub>4</sub> nanoparticles. *Mendeleev Communications* 20, 158–160. <https://doi.org/10.1016/j.mencom.2010.05.012>
- Romashkina, R.B., Majouga, A.G., Beloglazkina, E.K., Pichugina D.A., Askerka, M.S., Moiseeva, A.A., Rakhimov, R.D., Zyk, N.V., 2013. Sulfur-containing terpyridine derivatives: synthesis, coordination properties, and adsorption on the gold surface. *Russian Chemical Bulletin* 61, 2265–2281. <https://doi.org/10.1007/s11172-012-0322-0>
- Salimova, I.A., Berezina, A.V., Barskaya, E.S., Abramovich, M.S., Lyssenko K.A., Zyk, N.V., Beloglazkina, E.K., 2020. Syntheses of terpyridine-pyridylbenzothiazole linked ditopic ligands and their copper(II) complexes. *Polyhedron* 179, 114403. <https://doi.org/10.1021/ic900932j>
- Schäfer, B., Suryadevara, N., Greisch, J.-F., Fuhr, O., Kappes, M.M., Ruben, M., 2021. Ditopic Hexadentate Ligands with a Central Dihydrobenzo-diimidazole Unit Forming a [2x2] Zn<sub>4</sub> Grid Complex. *European Journal of Organic Chemistry* 2021(16), 2301-2310. <https://doi.org/10.1002/ejoc.202100230>
- Sierra, C., Castro Agudelo, B., Ochoa-Puentes, C., Rodriguez-Cordoba, W.Y., Reiber, A., 2018. Synthesis, characterization, X-ray crystal structure and DFT calculations of 4-([2,2':6',2''-terpyridin]-4'-yl)phenol. *Revista Colombiana de Química*. 47, 1.
- Shu, M., Tao, J., Han, Y., Fu, W., Li X., Zhang, R., Liu, J., 2022. Molecular engineering of terpyridine-Fe(II) coordination polymers consisting of quinoxaline-based  $\pi$ -spacers toward enhanced electrochromic performance. *Polymer* 256, 125231. <https://doi.org/10.1016/j.polymer.2022.125231>

Toledo, D., Baggio, R., Freire, E., Vega, A., Pizarro, N., Moreno, Y., 2015. Structure and spectroscopy of two new bases for building block: Terpyridine derivatives. *Journal of Molecular Structure* 1102, 18-24. <https://doi.org/10.1016/j.molstruc.2015.08.030>

Wang, H., Li, Y., Yu, H., Song, B., Lu, S., Hao, X.-Q., Zhang, Y., Wang, M., Hla, S.-W., Li, X., 2019. Combining synthesis and self-assembly in one pot to construct complex 2D Metallo-Supramolecules Using Terpyridine and Pyrylium Salts. *Journal of the American Chemical Society* 141(33), 13187–13195. <https://doi.org/10.1021/jacs.9b05682>

We,i C., He, Y., Shi, X., Song, Z., 2019. Terpyridine-metal complexes: Applications in catalysis and supramolecular chemistry. *Coordination Chemistry Reviews* 385, 1-19. <https://doi.org/10.1016/j.ccr.2019.01.005>

Yee, C.K., Ulman, A., Ruiz, J.D., Parikh, A., White, H., Rafailovich, M., 2003. Alkyl Selenide- and Alkyl Thiolate-Functionalized Gold Nanoparticles: Chain Packing and Bond Nature. *Langmuir* 19, 9450-9458. <https://doi.org/10.1021/la020628i>

Zibaseresht, R., 2019. Synthesis and characterization of a new ditopic bipyridine-

terpyridine bridging ligand using a Suzuki cross-coupling reaction. *Arkivoc* 2019, part vi. <https://doi.org/10.24820/ark.5550190.p011.044>

ISSN 1582-1021

e-ISSN 2668-4764

Edited by “Aurel Vlaicu” University of Arad  
Publishing House, Arad, Romania



Open Access

This article is licensed under a Creative Commons Attribution 4.0 International License, which permits use, sharing, adaptation, distribution and reproduction in any medium or format, as long as you give appropriate credit to the original author(s) and the source, provide a link to the Creative Commons license, and indicate if changes were made. The images or other third party material in this article are included in the article's Creative Commons license, unless indicated otherwise in a credit line to the material. If material is not included in the article's Creative Commons license and your intended use is not permitted by statutory regulation or exceeds the permitted use, you will need to obtain permission directly from the copyright holder.

To view a copy of this license, visit <http://creativecommons.org/licenses/by/4.0/>.

10.62591/Scien.Tech.Bull-Chem.FoodSci.Eng.2024.21.06